Sensor and Simulation Notes

Note 228

September 1977

Natural Frequencies and Capacitance of a Wire Above a Ground Plane and Capacitance of a Wire in a Parallel-Plate Region

F.C. Yang
G.C. Lewis, Jr.

Dikewood Corporation, Westwood Research Branch
Los Angeles, California

Abstract

The asymptotic antenna theory for a thin wire is used to obtain explicit analytical expressions for (i) the complex natural frequencies of a wire arbitrarily oriented above an infinite ground plane, (ii) the capacitance of a wire with respect to a ground plane, and (iii) the capacitance of a wire located in a parallel-plate region. Plots of these quantities are presented for several select cases.

ACKNOWLEDGEMENT

Thanks go to Drs. C.E. Baum, J.P. Castillo and K.C. Chen of the Air Force Weapons Laboratory for many enlightening discussions.

SECTION I
INTRODUCTION

Because of the relative ease with which one obtains large electromagnetic field strengths with parallel plates, parallel plates are used to simulate the effects of an electromagnetic pulse (EMP) on an aircraft or missile in flight. Obviously, the parallel plates interact with the test obstacle; and, therefore, the interaction between the plates and the test obstacle should be understood and qualified. To get some idea about what the interaction is, one may calculate and compare the complex natural frequencies and the capacitance of a test object in a free-flight environment and in a parallel-plate environment. These two quantities are calculated in refs. 1 and 2 with the test obstacle modeled as a cylindrical post, while refs. 3 and 4 give the natural frequencies and the transient response of a thin cylindrical wire arbitrarily oriented above an infinite, perfectly conducting plane (which is a special case of the two-parallel-plate geometry). The analyses in these references are based on the numerical solution of integral equations. More recently, an analytical approach using the asymptotic method; which was introduced to treat the thin-wire problem in the early twentieth century, is reported in ref. 5, together with some calculations on the natural frequencies and the transient responses of several thin-wire structures. The results obtained therein are so simple that it is tempting to apply this method to the problem depicted in figure 1.

Based on the approach given in ref. 5, the complex natural frequencies are calculated in section II for a thin cylindrical wire arbitrarily oriented above an infinite, perfectly conducting plane (figure 1). The more general case of two parallel plates is left for future consideration. In section III, the capacitances of a wire above a ground plane and between two parallel plates are calculated. This quantity is certainly very useful to characterize the low-frequency interaction between the wire and the simulator if the wire is excited by the so-called current injection method.

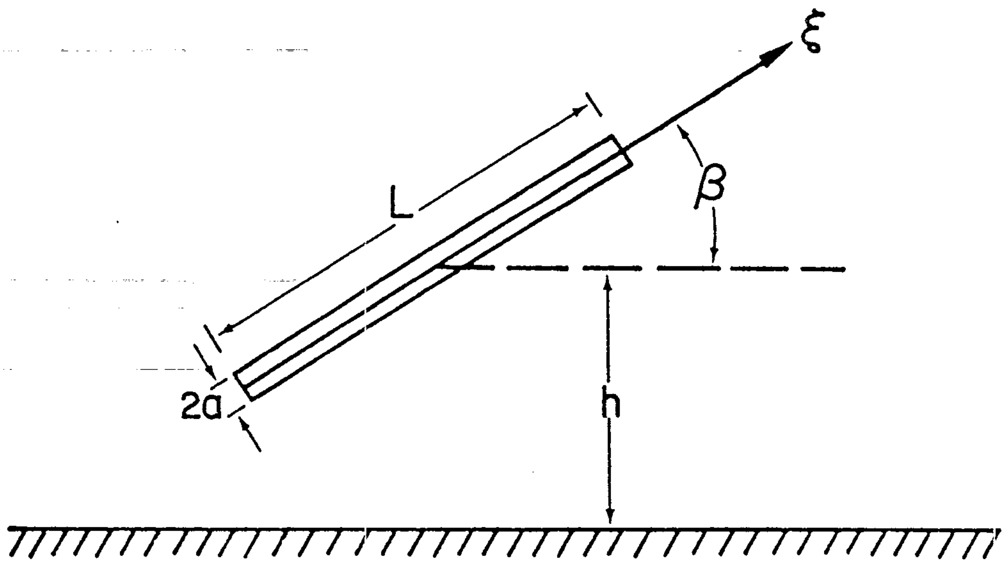

Figure 1. A wire above an infinite ground plane.

SECTION II

COMPLEX NATURAL FREQUENCIES

In this section, the asymptotic method is used to calculate the complex natural frequencies of the geometry shown in figure 1 which depicts a cylindrical wire arbitrarily oriented above an infinite, perfectly conducting plane. The radius of this wire is assumed to be small compared to the shortest distance between the wire and the conducting plane as well as the length of the wire. Under this thin-wire assumption, the total current $I(\xi)$ flowing along the wire satisfies the following integro-differential equation (refs. 3 and 4):

$$\int_0^L I(\xi')\{\mathcal{L}_o G_o(\xi,\xi') + \mathcal{L}_1 G_1(\xi,\xi')\}d\xi' = -s\varepsilon_o E_\xi^{inc}(\xi) \qquad (1)$$

where

$$\mathcal{L}_o = \frac{\partial^2}{\partial\xi^2} - \frac{s^2}{c^2}$$

$$\mathcal{L}_1 = \frac{\partial^2}{\partial\xi\partial\xi'} + \frac{s^2}{c^2}\cos 2\beta$$

$$G_o(\xi,\xi') = \frac{e^{-s[(\xi-\xi')^2 + a^2]^{1/2}/c}}{4\pi[(\xi-\xi')^2 + a^2]^{1/2}}$$

$$G_1(\xi,\xi') = \frac{e^{-s\{[(L-\xi-\xi')\sin\beta - 2h]^2 + [(\xi-\xi')\cos\beta]^2\}^{1/2}/c}}{4\pi\{[(L-\xi-\xi')\sin\beta - 2h]^2 + [(\xi-\xi')\cos\beta]^2\}^{1/2}}$$

$$c = (\mu_o\varepsilon_o)^{-1/2} = \text{speed of light}$$

and E_ξ^{inc} is the tangential component of the incident electric field on the wire.

To solve equation (1) by the asymptotic method, the first step is to integrate equation (1) and to obtain the following equation:

$$\int_0^L I(\xi') \frac{e^{-s[(\xi-\xi')^2 + a^2]^{\frac{1}{2}}/c}}{4\pi[(\xi-\xi')^2 + a^2]^{\frac{1}{2}}} d\xi' = \frac{A}{4\pi} \sinh(s\xi/c) + \frac{B}{4\pi} \cosh(s\xi/c)$$

$$- \frac{c}{s} \int_0^\xi \int_0^L I(\xi')\sinh[s(\xi-\xi'')/c] \left[\frac{\partial^2}{\partial\xi''\partial\xi'} + \frac{s^2}{c^2} \cos 2\beta\right] G_1(\xi'',\xi')d\xi' d\xi'' \tag{2}$$

$$- c\varepsilon_0 \int_0^\xi E_\xi^{inc}(\xi')\sinh[s(\xi-\xi')/c]d\xi'$$

where A and B are integration constants determined from the end conditions $I(0) = I(L) = 0$. Next, the left-hand side integral is approximated by

$$\int_0^L I(\xi') \frac{e^{-s[(\xi-\xi')^2 + a^2]^{\frac{1}{2}}/c}}{4\pi[(\xi-\xi')^2 + a^2]^{\frac{1}{2}}} d\xi' \approx \frac{\Omega}{4\pi} I(\xi) + \frac{1}{4\pi} \ell n[4\xi(L-\xi)/L^2]I(\xi)$$

$$+ \int_0^L \frac{I(\xi')e^{-s|\xi-\xi'|/c} - I(\xi)}{4\pi|\xi-\xi'|} d\xi' + 0(\Omega^{-1}) \tag{3}$$

with $\Omega = 2 \ell n(L/a)$.

Equations (2) and (3) combined with the end condition $I(0) = 0$ result in the following equation:

$$I(\xi)\{1 + \Omega^{-1}\ell n[4(L-\xi)\xi/L^2]\} + \Omega^{-1} \int_0^L \frac{I(\xi')e^{-s|\xi-\xi'|/c} - I(\xi)}{|\xi-\xi'|} d\xi'$$

$$= A\Omega^{-1}\sinh(s\xi/c) + \Omega^{-1}\cosh(s\xi/c) \int_0^L \frac{I(\xi')e^{-s\xi'/c}}{\xi'} d\xi'$$

$$- 4\pi c\varepsilon_o \Omega^{-1} \int_0^{\xi} E_{\xi}^{inc}(\xi')\sinh[s(\xi-\xi')/c]d\xi' \qquad (4)$$

$$- \Omega^{-1} 4\pi c s^{-1} \int_0^{\xi}\int_0^{L} I(\xi')\sinh[s(\xi-\xi'')/c]\left[\frac{\partial^2}{\partial\xi''\partial\xi'} + \frac{s^2}{c^2}\cos 2\beta\right] G_1(\xi'',\xi')d\xi' d\xi''$$

which together with the other end condition $I(L) = 0$ gives

$$\int_0^L \frac{I(\xi')e^{-s(L-\xi')/c}}{L-\xi'} d\xi' = A\sinh(sL/c) + \cosh(sL/c)\int_0^L \frac{I(\xi')e^{-s\xi'/c}}{\xi'} d\xi'$$

$$- \frac{4\pi c}{s}\int_0^L\int_0^L I(\xi')\sinh[s(L-\xi'')/c]\left[\frac{\partial^2}{\partial\xi''\partial\xi'} + \frac{s^2}{c^2}\cos 2\beta\right] G_1(\xi'',\xi')d\xi' d\xi'' \qquad (5)$$

$$- 4\pi c\varepsilon_o \int_0^L E_{\xi}^{inc}(\xi')\sinh[s(L-\xi')/c]d\xi'$$

Although A can be eliminated from equations (4) and (5), the removal of A leads one in an unproductive direction. It is preferable to keep equations (4) and (5) as they are.

The complex frequency s_n and the corresponding current distribution $I_n(\xi)$ of the n-th natural mode are obtained by finding the nontrivial solutions of the homogeneous equations (4) and (5), i.e., by setting $E_{\xi}^{inc}(\xi) \equiv 0$ in these equations. However, before one solves these homogeneous equations, the constant A is set equal to $- i\Omega$. If one recalls that $I_n(\xi)$ is determined only within a multiplicative constant, the reason for setting $A = - i\Omega$ is apparent when $I_n(\xi)$ is obtained.

The asymptotic method is now applied to the homogeneous equations (4) and (5). First, assume the following asymptotic expansions in powers of Ω^{-1}

$$s = s_o + s_1\Omega^{-1} + \ldots$$
$$I = I_o + I_1\Omega^{-1} + \ldots \tag{6}$$

Then, substituting these expansions into the homogeneous equations (4) and (5), one finally obtains

$$\frac{L}{c} s_n = in\pi + \Omega^{-1}F_n(\beta,\eta) + O(\Omega^{-2})$$
$$I_n(\xi) = \sin(n\pi\xi/L) + O(\Omega^{-1}) \tag{7}$$

where

$$F_n(\beta,\eta) = - E(2n\pi)$$
$$- \frac{i}{n\pi}\int_0^1\int_0^1 \sin(n\pi\xi'')\sin(n\pi\xi')\left[\frac{\partial^2}{\partial\xi''\partial\xi'} - n^2\pi^2\cos 2\beta\right]\frac{e^{-in\pi R(\xi'',\xi')}}{R(\xi'',\xi')}\,d\xi' d\xi''$$

$$R(\xi'',\xi') = \left\{[(1-\xi''-\xi')\sin\beta - \eta]^2 + [(\xi''-\xi')\cos\beta]^2\right\}^{\frac{1}{2}}$$

$$\eta = 2h/L$$

$$E(z) = \int_0^z [1 - \exp(- i\xi)]\xi^{-1}d\xi$$
$$= \gamma + \ell n\, z - Ci(z) + i\,Si(z)$$

$\gamma = 0.5772 =$ Euler's constant

and $Ci(z)$, $Si(z)$ are, respectively, the cosine and sine integrals (ref. 6).

As can be seen from equation (7), the leading term of $I_n(\xi)$ is $\sin(n\pi\xi/L)$ and s_n is expressed in terms of a double integral. By introducing a suitable coordinate transformation the double integral is reduced to a single integral, i.e.,

$$F_n(\beta,\eta) = -E(2n\pi) + \frac{\sin\beta}{2}\int_0^{\theta_o}\left\{\frac{\exp[-in\pi\rho(\cos\beta - \sin\theta)]}{\cos\beta - \sin\theta} + \frac{\exp[-in\pi\rho(\cos\beta + \sin\theta)]}{\cos\beta + \sin\theta}\right\}_{\rho_1}^{\rho_2} d\theta$$

$$+ (-1)^n \frac{\cos\beta}{2}\int_0^{\theta_o}\left\{\frac{\exp\left(in\pi[\eta - \rho\cos\beta(\sin\beta + \cos\theta)]/\sin\beta\right)}{\sin\beta + \cos\theta} + \frac{\exp\left(-in\pi[\eta + \rho\cos\beta(\sin\beta - \cos\theta)]/\sin\beta\right)}{\sin\beta - \cos\theta}\right\}_{\rho_1}^{\rho_2} d\theta \qquad (8)$$

where

$$\theta_o = \tan^{-1}(\cos\beta/\eta)$$

$$\rho_2 = (\eta + \sin\beta)/\cos(\theta - \beta)$$

$$\rho_1 = (\eta - \sin\beta)/\cos(\theta + \beta)$$

For the special case of $\beta = 0°$, $F_n(0,\eta)$ can be integrated to yield

$$F_n(0,\eta) = -E(2n\pi) - 2E(n\pi\eta) + E[n\pi\sqrt{1+\eta^2} + 1] + E[n\pi\sqrt{1+\eta^2} - 1] \qquad (9)$$

which agrees with the result presented in ref. 5. For the other special case where $\beta = \pi/2$, the integral can also be carried out to give

$$F_n(\pi/2,\ \eta) = -E(2n\pi) + (-1)^n i\sin(n\pi\eta)\,\ell n[\eta^2/(\eta^2 - 1)] + \frac{(-1)^n}{2}\exp(in\pi\eta)\left[E\left(2n\pi(\eta-1)\right) + E\left(2n\pi(\eta+1)\right) - 2E(2n\pi\eta)\right] \qquad (10)$$

which, apart from the factor $(-1)^n$ in the last two terms of equation (10) is similar to the result that is given in ref. 5.- For the general case of an arbitrary wire orientation, the integral is evaluated numerically by using Simpson's rule. Several numerical results are given in figures 2 - 9. However, it should be mentioned that the region where $\eta - \sin\beta \ll 1$ is excluded from the figures. The reason is that when $\eta - \sin\beta \ll 1$ the interaction between the wire and the ground plane becomes so strong that the asymptotic approach is no longer valid.

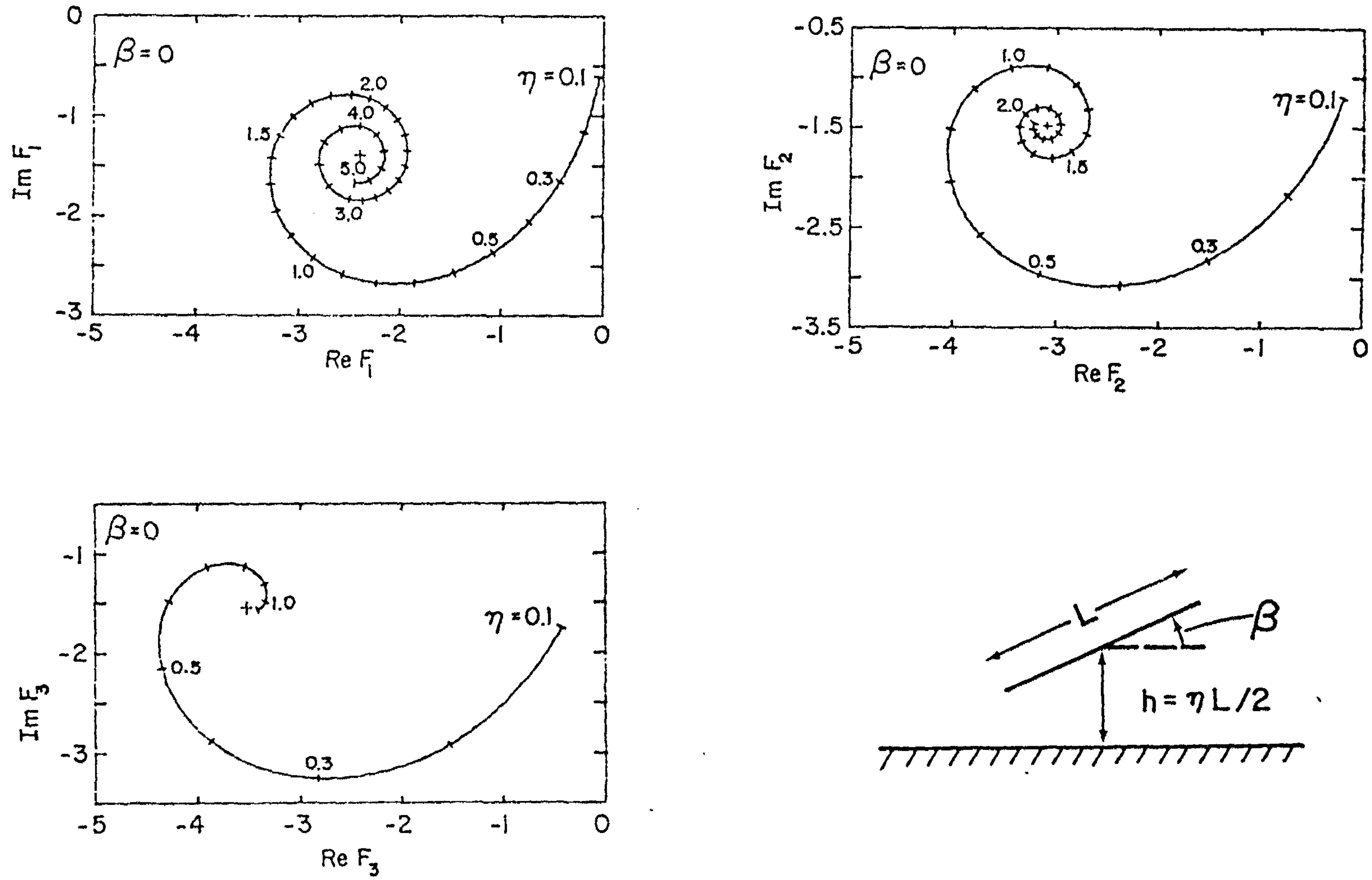

Figure 2. Variation with $\eta = 2h/L$ of the functions $F_n(\beta,\eta)$ $(n = 1,2,3)$ defined by equation (7) for $\beta = 0$. The + sign denotes $F_n(\beta,\infty)$. The complex natural frequency s_n of the n^{th} resonance is given by $s_n = in\pi c/L + (c/L\Omega)F_n(\beta,\eta)$.

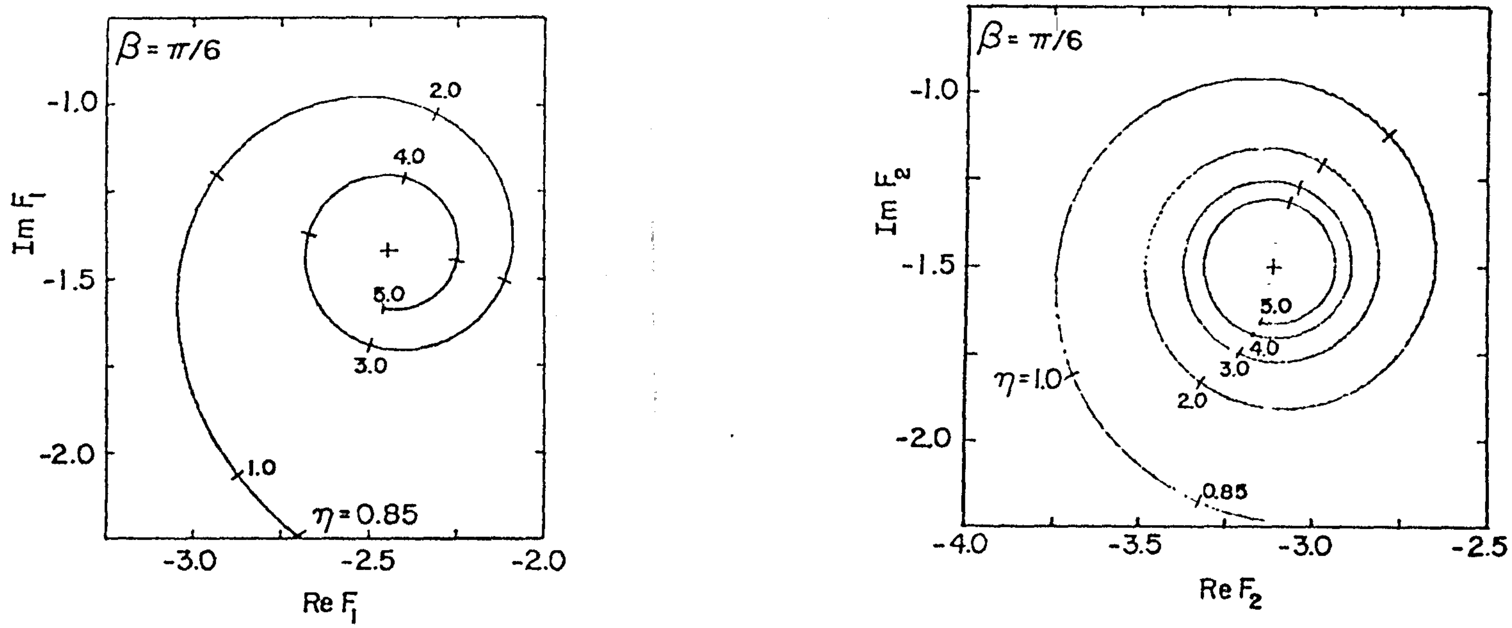

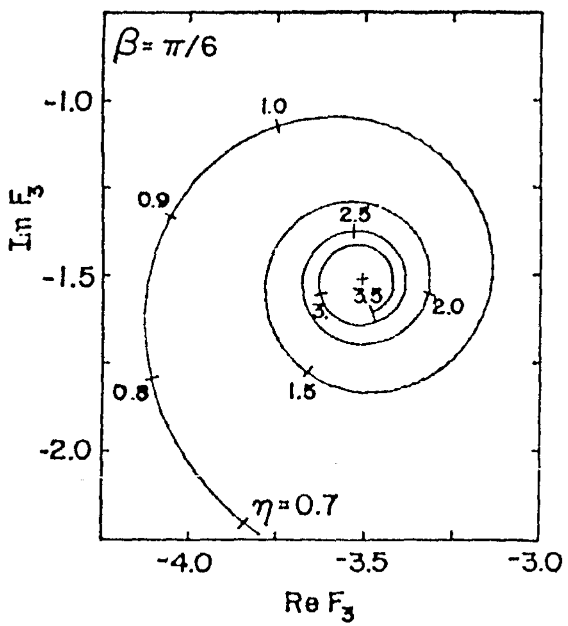

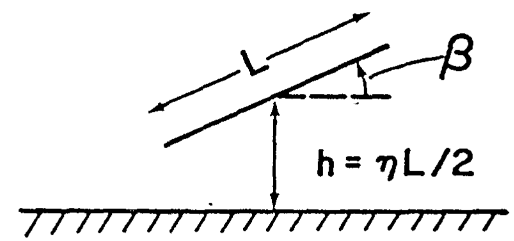

Figure 3. Variation with $\eta = 2h/L$ of the functions $F_n(\beta,\eta)$ $(n = 1,2,3)$ defined by equation (7) for $\beta = \pi/6$. The + sign denotes $F_n(\beta,\infty)$. The complex natural frequency s_n of the n^{th} resonance is given by $s_n = in\pi c/L + (c/L\Omega)F_n(\beta,\eta)$.

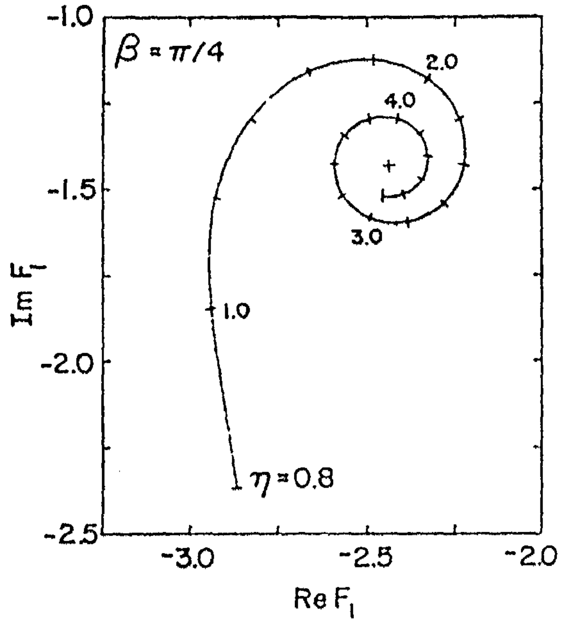

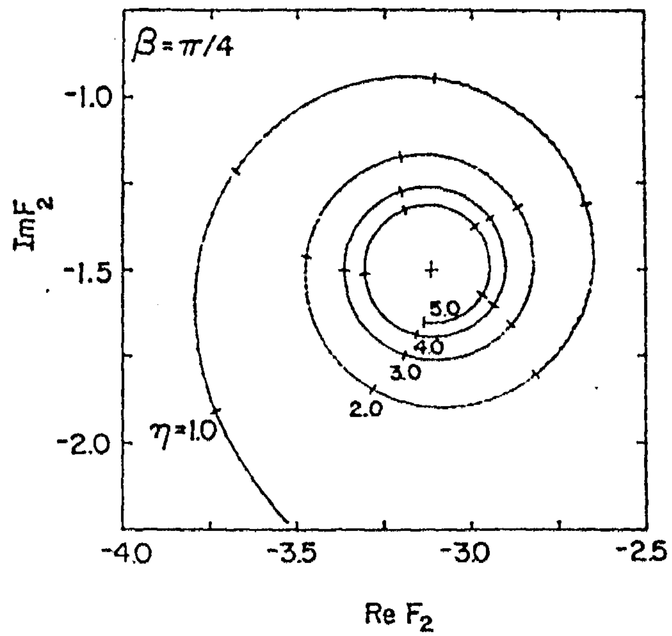

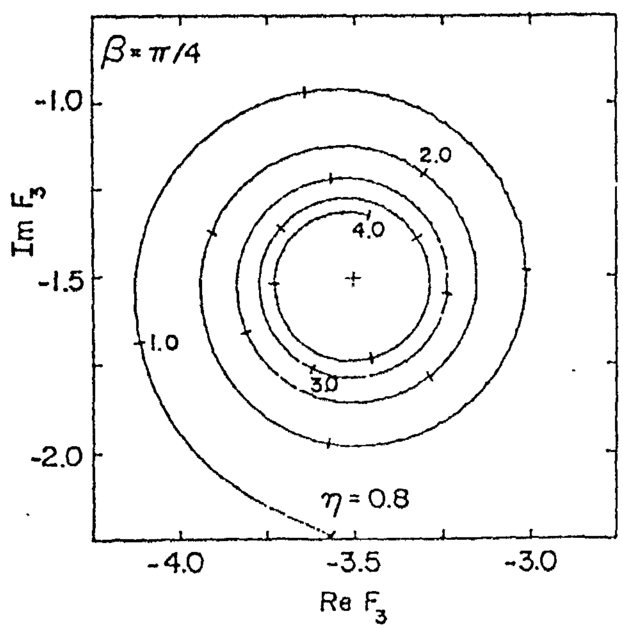

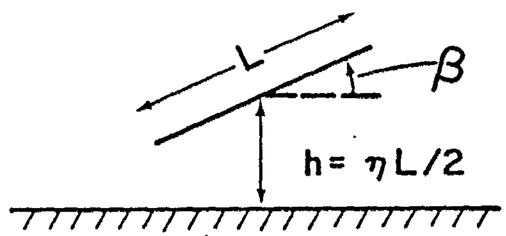

Figure 4. Variation with $\eta = 2h/L$ of the functions $F_n(\beta,\eta)$ $(n = 1,2,3)$ defined by equation (7) for $\beta = \pi/4$. The + sign denotes $F_n(\beta,\infty)$. The complex natural frequency s_n of the n^{th} resonance is given by $s_n = in\pi c/L + (c/L\Omega)F_n(\beta,\eta)$.

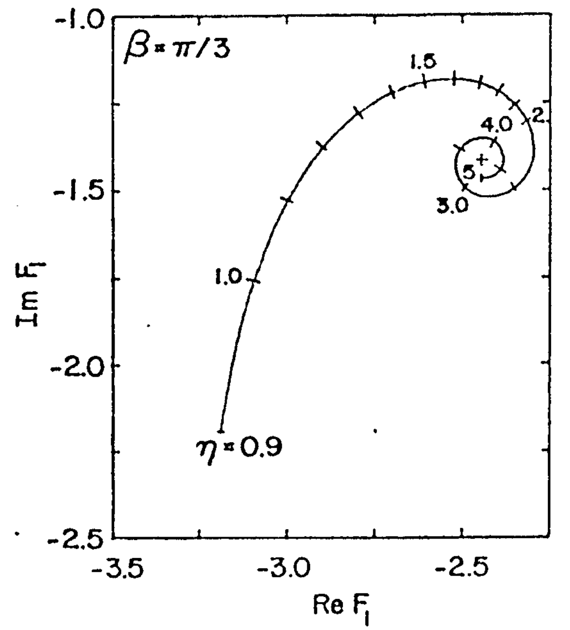

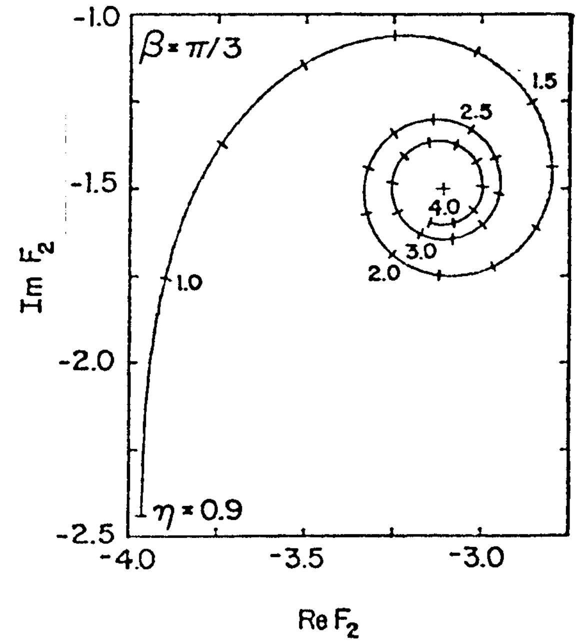

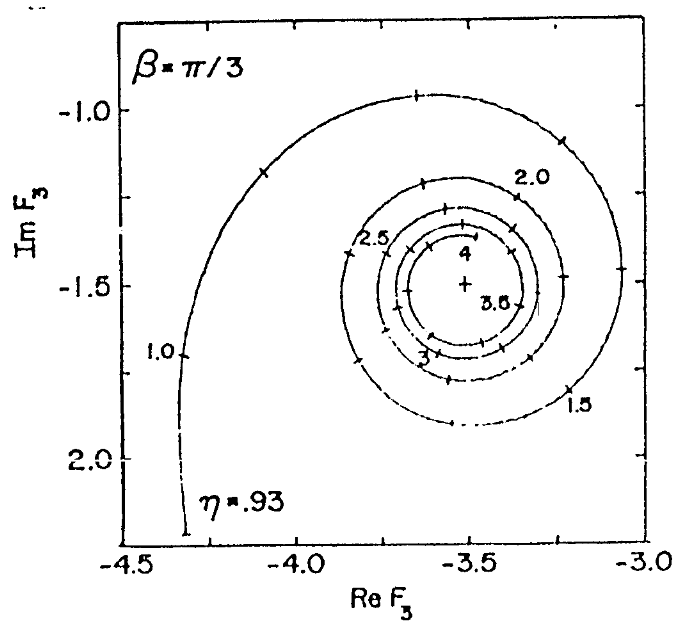

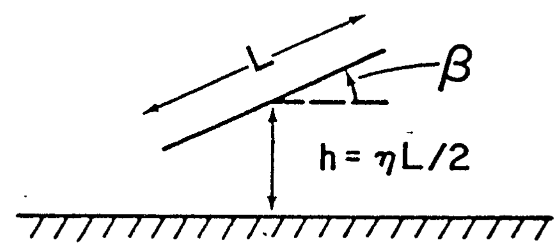

Figure 5. Variation with $\eta = 2h/L$ of the functions $F_n(\beta,\eta)$ $(n = 1,2,3)$ defined by equation (7) for $\beta = \pi/3$. The + sign denotes $F_n(\beta,\infty)$. The complex natural frequency s_n of the n^{th} resonance is given by $s_n = in\pi c/L + (c/L\Omega)F_n(\beta,\eta)$.

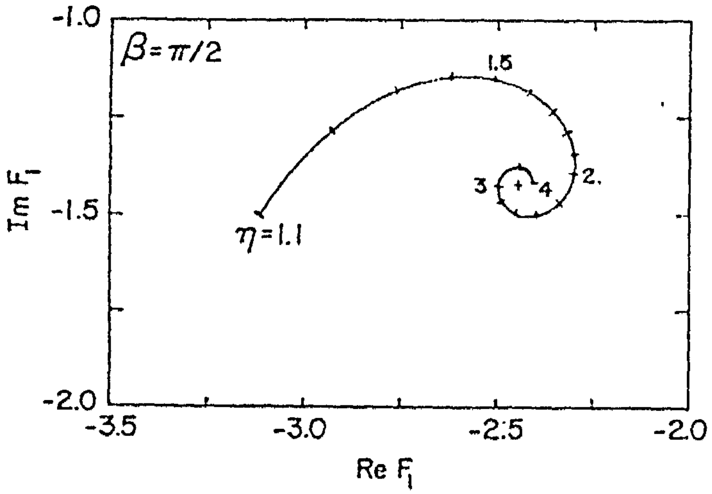

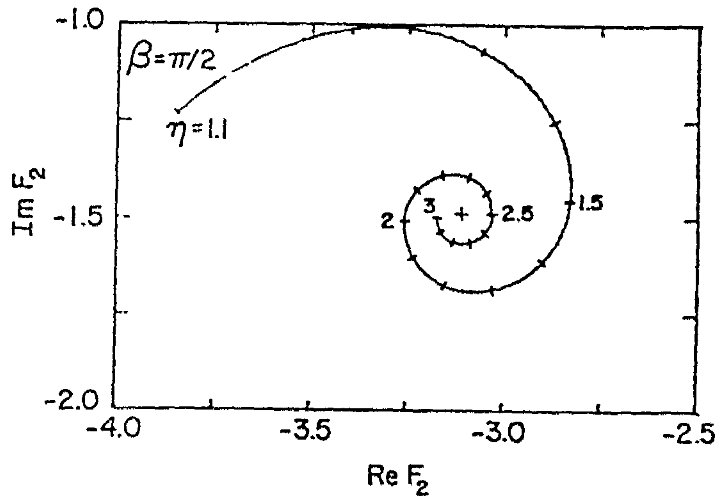

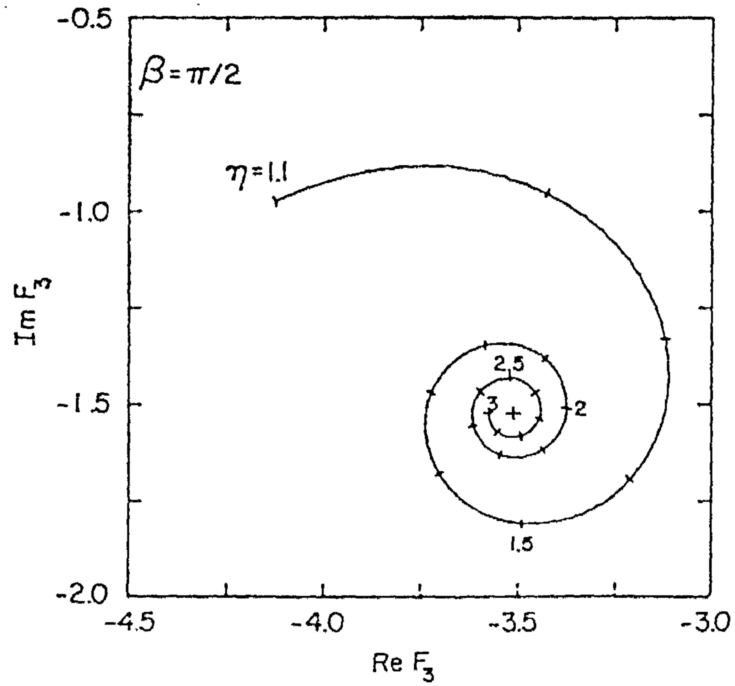

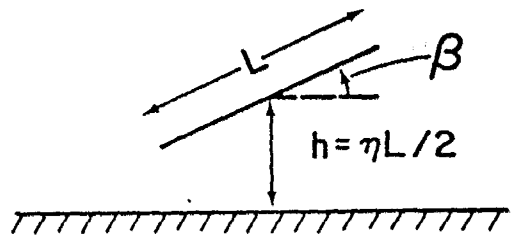

Figure 6. Variation with $\eta = 2h/L$ of the functions $F_n(\beta,\eta)$ $(n = 1,2,3)$ defined by equation (7) for $\beta = \pi/2$. The + sign denotes $F_n(\beta,\infty)$. The complex natural frequency s_n of the n^{th} resonance is given by $s_n = in\pi c/L + (c/L\Omega)F_n(\beta,\eta)$.

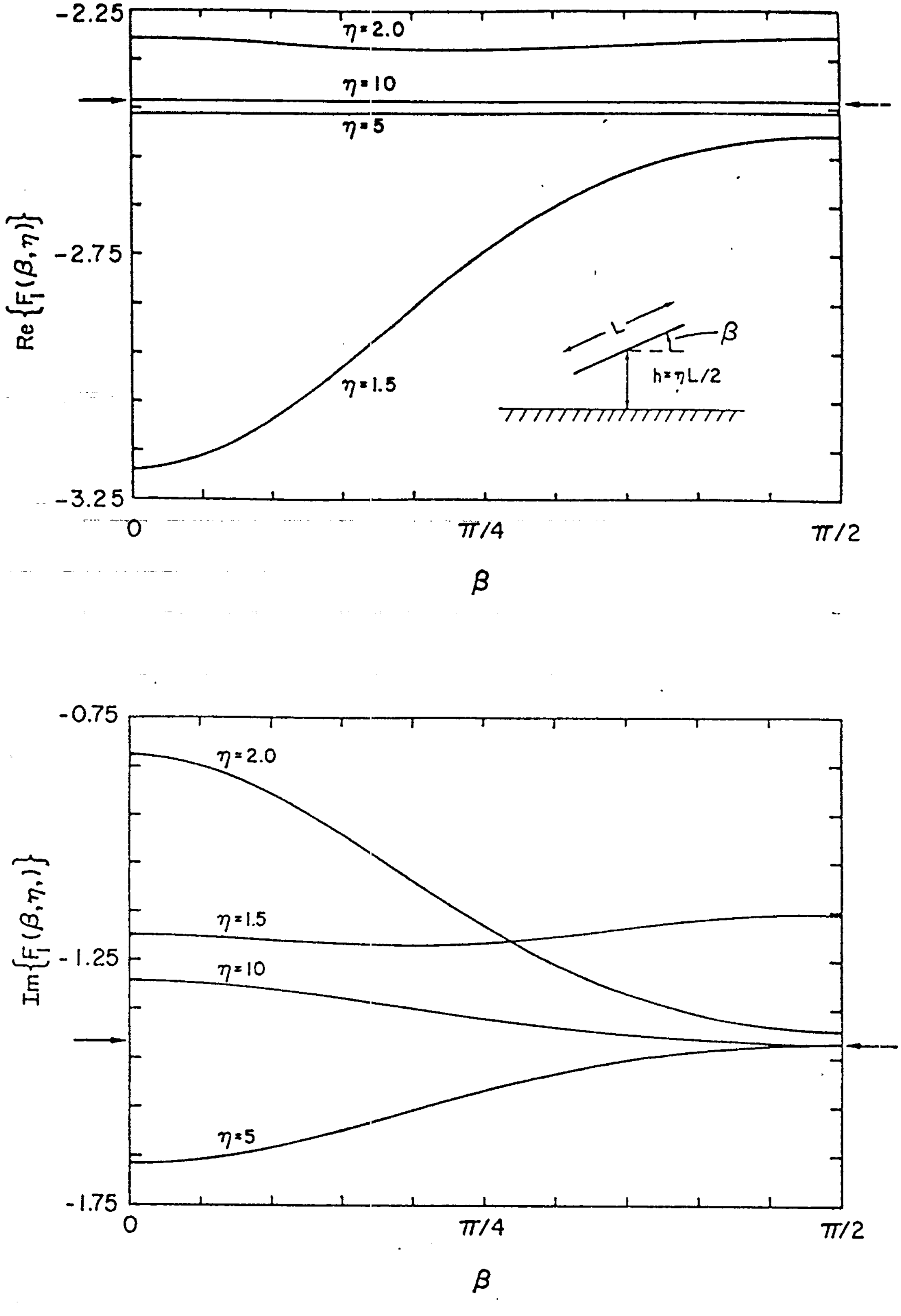

Figure 7. Variation with β of the function $F_1(\beta,\eta)$ for $\eta = 2h/L = 1.5, 2, 5, 10$. The arrows denote the value of $F_1(\beta,\infty)$.

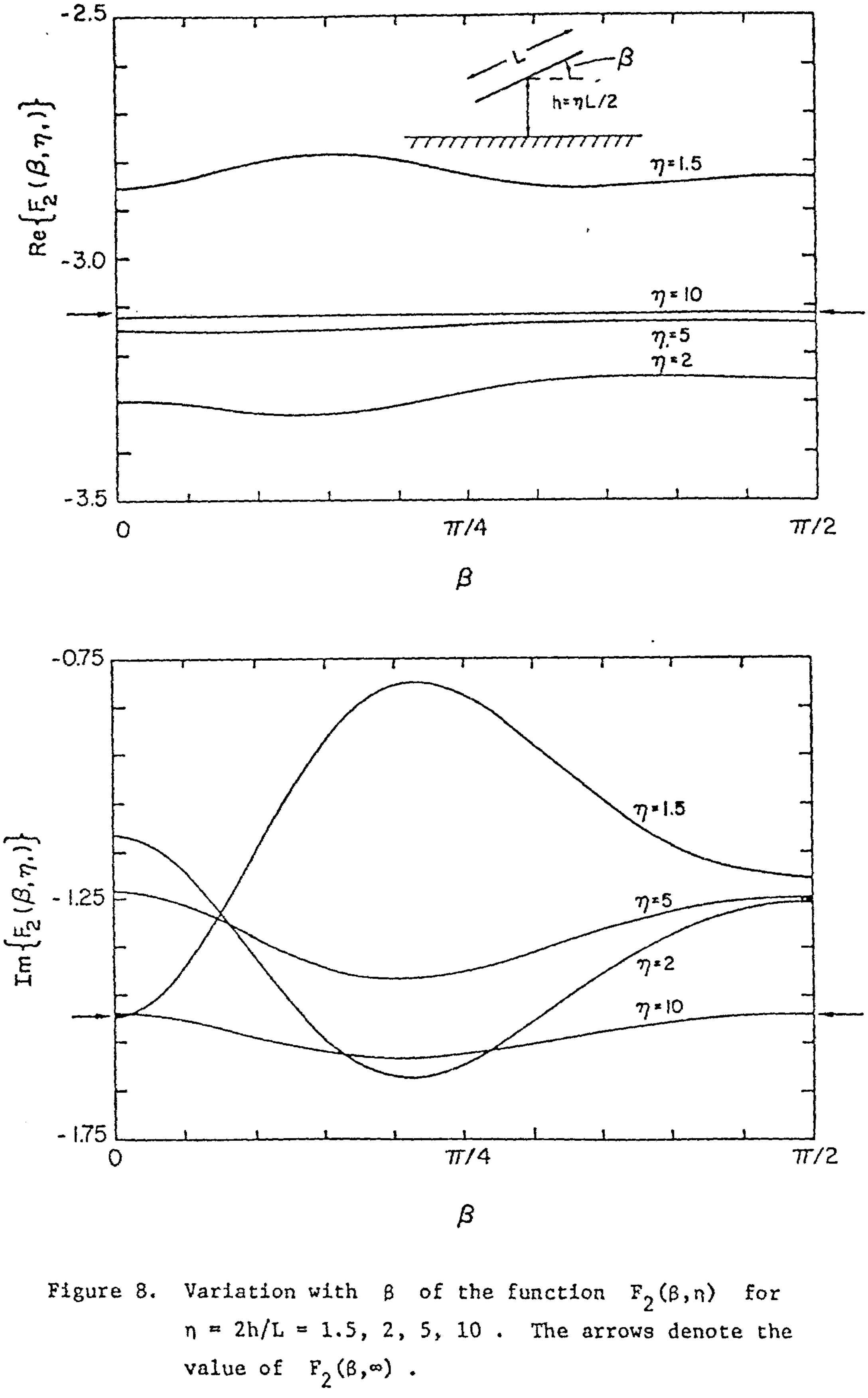

Figure 8. Variation with β of the function $F_2(\beta,\eta)$ for $\eta = 2h/L = 1.5, 2, 5, 10$. The arrows denote the value of $F_2(\beta,\infty)$.

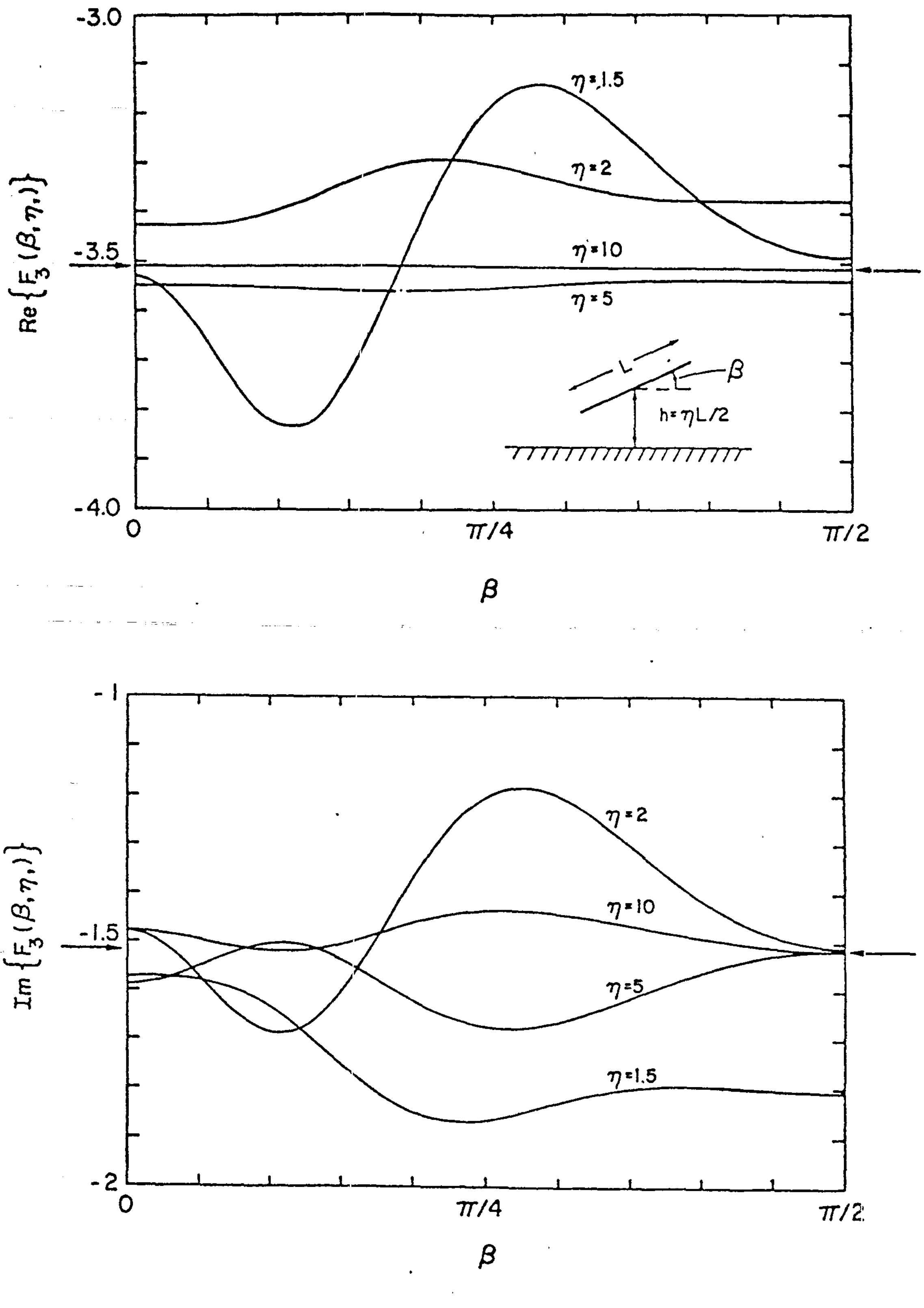

Figure 9. Variation with β of the function $F_3(\beta,\eta)$ for $\eta = 2h/L = 1.5, 2, 5, 10$. The arrows denote the value of $F_3(\beta,\infty)$.

SECTION III
CAPACITANCES

The capacitance of a wire with respect to two parallel plates is calculated in this section by the low-frequency version of the asymptotic approach. The capacitance of the wire-single plate geometry as shown in figure 1 can then be obtained by removing one of the two plates of figure 10.

To calculate the capacitance of the structure in figure 10, one assumes a constant potential V_o on the wire. Then, the linear charge distribution $\tau(\xi)$ satisfies the following equation

$$\int_o^L \tau(\xi')\left[\sum_{n=-\infty}^{\infty} \frac{1}{R_n^{(2)}} - \sum_{n=-\infty}^{\infty} \frac{1}{R_n^{(1)}}\right]d\xi' = 4\pi\varepsilon_o V_o \tag{11}$$

with

$$R_n^{(2)} = \left\{[(\xi-\xi')\sin\beta - 2nd]^2 + [(\xi-\xi')\cos\beta]^2\right\}^{\frac{1}{2}}, \qquad n \neq 0$$

$$R_o^{(2)} = [(\xi-\xi')^2 + a^2]^{\frac{1}{2}}$$

$$R_n^{(1)} = \left\{[(L-\xi-\xi')\sin\beta - 2(h+nd)]^2 + [(\xi-\xi')\cos\beta]^2\right\}^{\frac{1}{2}}$$

Similar to section II, the asymptotic method is now used to solve equation (11). Substituting the following relations into equation (11)

$$\int_o^L \frac{\tau(\xi')d\xi'}{\sqrt{(\xi-\xi')^2 + a^2}} \approx \Omega\,\tau(\xi) + \ell n\,[4\xi(L-\xi)/L^2]\tau(\xi) + \int_o^L \frac{\tau(\xi') - \tau(\xi)}{|\xi-\xi'|}\,d\xi'$$

$$\tau(\xi) = \Omega^{-1}\tau_1(\xi) + \Omega^{-2}\tau_2(\xi)$$

one immediately obtains

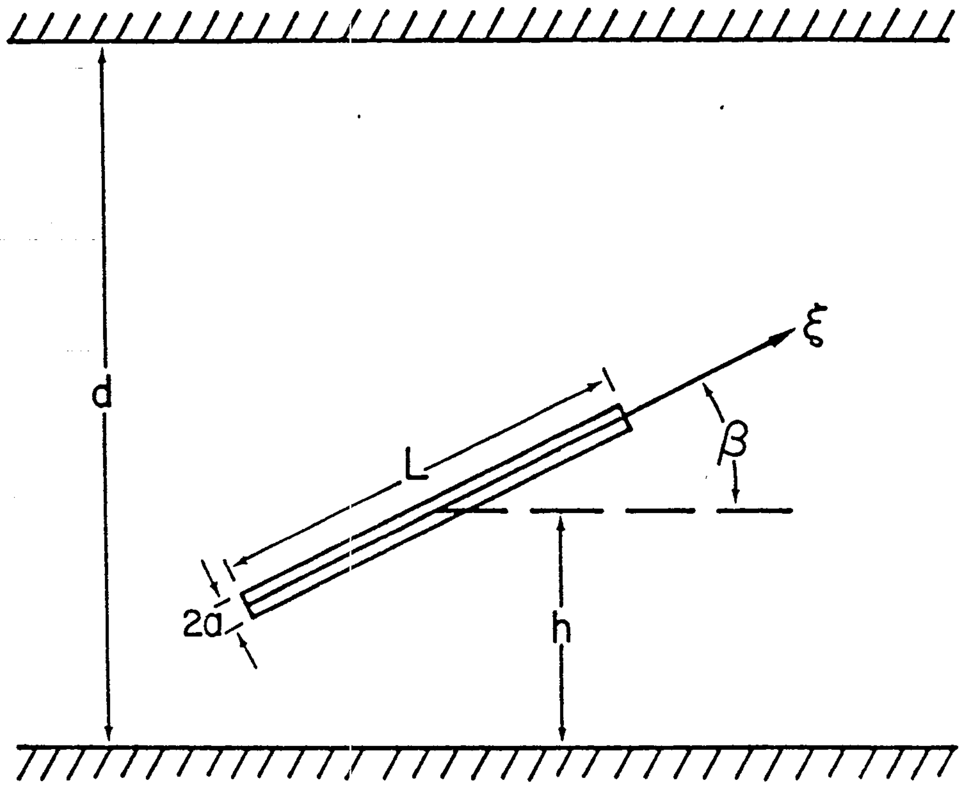

Figure 10. A wire located in a parallel-plate region.

$$\tau_1(\xi) = 4\pi\varepsilon_o V_o$$

$$\tau_2(\xi) = -4\pi\varepsilon_o V_o \left\{ \ell n[4\xi(L-\xi)/L^2] + \int_o^L \left[\sum_{\substack{n=-\infty \\ n\neq 0}}^{n=\infty} \frac{1}{R_n^{(2)}} - \sum_{n=-\infty}^{n=\infty} \frac{1}{R_n^{(1)}} \right] d\xi' \right\} \tag{12}$$

The capacitance of the geometry shown in figure 10 is then given by

$$C = \int_o^L \tau(\xi) d\xi / V_o \tag{13.a}$$

$$\simeq \frac{4\pi\varepsilon_o L}{\Omega} \left[1 - \frac{1}{\Omega} (\ell n\ 4 - 2 - C_p) \right]$$

with

$$C_p = \frac{1}{L} \left[\sum_{n=-\infty}^{n=\infty} \int_o^L \int_o^L \frac{d\xi' d\xi}{R_n^{(1)}} - \sum_{\substack{n=-\infty \\ n\neq 0}}^{n=\infty} \int_o^L \int_o^L \frac{d\xi' d\xi}{R_n^{(2)}} \right] \tag{13.b}$$

$$= \sum_{n=0}^{\infty} C_{pn}^{(1)} - \sum_{n=1}^{n=\infty} C_{pn}^{(2)}$$

$$C_{po}^{(1)} = \frac{\eta}{\sin\beta} \ell n \left[\frac{(1+\sin\beta)(1-\sin\beta\sqrt{1+\cos^2\beta/\eta^2})}{(1-\sin\beta)(1+\sin\beta\sqrt{1+\cos^2\beta/\eta^2})} \right]$$

$$+ \ell n \frac{\sqrt{\eta^2+\cos^2\beta}+1}{\sqrt{\eta^2+\cos^2\beta}-1}$$

$$C_{pn}^{(1)} = \frac{\eta+n\Delta}{\sin\beta} \ell n \left\{ \frac{(1+\sin\beta)[1-\sin\beta\sqrt{1+\cos^2\beta/(\eta+n\Delta)^2}]}{(1-\sin\beta)[1+\sin\beta\sqrt{1+\cos^2\beta/(\eta+n\Delta)^2}]} \right\} \qquad \text{for} \quad n \neq 0$$

$$+ \frac{\eta - n\Delta}{\sin\beta} \ln \left\{ \frac{(1-\sin\beta)[1+\sin\beta\sqrt{1+\cos^2\beta/(\eta-n\Delta)^2}]}{(1+\sin\beta)[1-\sin\beta\sqrt{1+\cos^2\beta/(\eta-n\Delta)^2}]} \right\} \qquad \text{for} \quad n \neq 0$$

$$+ \ln \frac{\sqrt{(\eta+n\Delta)^2 + \cos^2\beta} + 1}{\sqrt{(\eta+n\Delta)^2 + \cos^2\beta} - 1} + \ln \frac{\sqrt{(n\Delta-\eta)^2 + \cos^2\beta} + 1}{\sqrt{(n\Delta-\eta)^2 + \cos^2\beta} - 1}$$

$$C_{pn}^{(2)} = 2(1 - n\Delta\sin\beta)\ln\left[\frac{\sqrt{(1-n\Delta\sin\beta)^2 + (n\Delta\cos\beta)^2} + (1-n\Delta\sin\beta)}{(1-\sin\beta)n\Delta}\right]$$

$$+2(1 + n\Delta\sin\beta)\ln\left[\frac{\sqrt{(1+n\Delta\sin\beta)^2 + (n\Delta\cos\beta)^2} + (1+n\Delta\sin\beta)}{(1+\sin\beta)n\Delta}\right]$$

$$-2\left[\sqrt{(1-n\Delta\sin\beta)^2 + (n\Delta\cos\beta)^2} - n\Delta\right]$$

$$-2\left[\sqrt{(1+n\Delta\sin\beta)^2 + (n\Delta\cos\beta)^2} - n\Delta\right]$$

and

$$\Delta = 2d/L > 2h/L = \eta > \sin\beta$$

When $\eta \gg 1$ and $\Delta - \eta \gg 1$, equation (13.b) is approximated by

$$C_p \approx \eta^{-1} + \Delta^{-1}[2\psi(1) - \psi(1+\eta/\Delta) - \psi(1-\eta/\Delta)]$$

where $\psi(x)$ is the Psi function (ref. 6).

For the special cases of $\beta = 0°$ and $90°$, all the C_{pn}'s are simplified and are given by

(i) for $\beta = 0°$

$$C_{po}^{(1)} = -2(\sqrt{\eta^2+1} - \eta) + 2\ln(\sqrt{1+\eta^{-2}} + \eta^{-1})$$

$$C_{pn}^{(1)} = -2(\eta+n\Delta)\left[\sqrt{1+(\eta+n\Delta)^{-2}} - 1\right] + 2\ln\left[\sqrt{1+(\eta+n\Delta)^{-2}} + (\eta+n\Delta)^{-1}\right]$$

$$+ 2(\eta - n\Delta)\left[\sqrt{1 + (\eta - n\Delta)^{-2}} - 1\right] + 2\ \ell n\left[\sqrt{1 + (\eta - n\Delta)^{-2}} - (\eta - n\Delta)^{-1}\right], \quad n \neq 0$$

$$C_{pn}^{(2)} = 4\ \ell n\left[\sqrt{1 + (n\Delta)^{-2}} + (n\Delta)^{-1}\right] - 4\left[\sqrt{1 + (n\Delta)^{2}} - n\Delta\right] \tag{14.a}$$

(ii) for $\beta = 90°$

$$C_{po}^{(1)} = \eta\ \ell n(1 - \eta^{-2}) + \ell n[(\eta + 1)/(\eta - 1)]$$

$$C_{pn}^{(1)} = (\eta + n\Delta)\ell n[1 - (\eta + n\Delta)^{-2}] + \ell n[(\eta + n\Delta + 1)/(\eta + n\Delta - 1)]$$

$$- (\eta - n\Delta)\ell n[1 - (\eta - n\Delta)^{-2}] + \ell n[(n\Delta - \eta + 1)/(n\Delta - \eta - 1)], \quad n \neq 0$$

$$C_{pn}^{(2)} = 2(1 + n\Delta)\ell n[1 + (n\Delta)^{-1}] + 2(n\Delta - 1)\ell n[1 - (n\Delta)^{-1}] \tag{14.b}$$

To calculate the capacitances of the wire-single plate geometry shown in figure 1, one takes the limit $\Delta - \eta \to \infty$ in equation (13) and obtains

$$C_p(\Delta - \eta \to \infty) \simeq C_{po}^{(1)}$$

$$= \frac{\eta}{\sin\beta}\ \ell n\left[\frac{(1 + \sin\beta)(1 - \sin\beta\sqrt{1 + \cos^2\beta/\eta^2})}{(1 - \sin\beta)(1 + \sin\beta\sqrt{1 + \cos^2\beta/\eta^2})}\right] + \ell n\ \frac{\sqrt{\eta^2 + \cos^2\beta} + 1}{\sqrt{\eta^2 + \cos^2\beta} - 1} \tag{15}$$

which reduces to η^{-1} when $\eta >> 1$.

Several numerical examples of C_p are shown in figures 11 - 13. It is noticed that the result agrees with that of ref. 2 where the special case of $\beta = \pi/2$, $\Delta - \eta \to \infty$ is considered. Finally we mention that

$$\frac{1}{\Omega} C_p \simeq \frac{C - C_\infty}{C_\infty} \tag{16}$$

where C_∞ is the capacitance of a wire in free space,

$$C_\infty \simeq \frac{4\pi\varepsilon_o L}{\Omega}\left[1 + \frac{1}{\Omega}(2 - \ell n\ 4)\right] \tag{17}$$

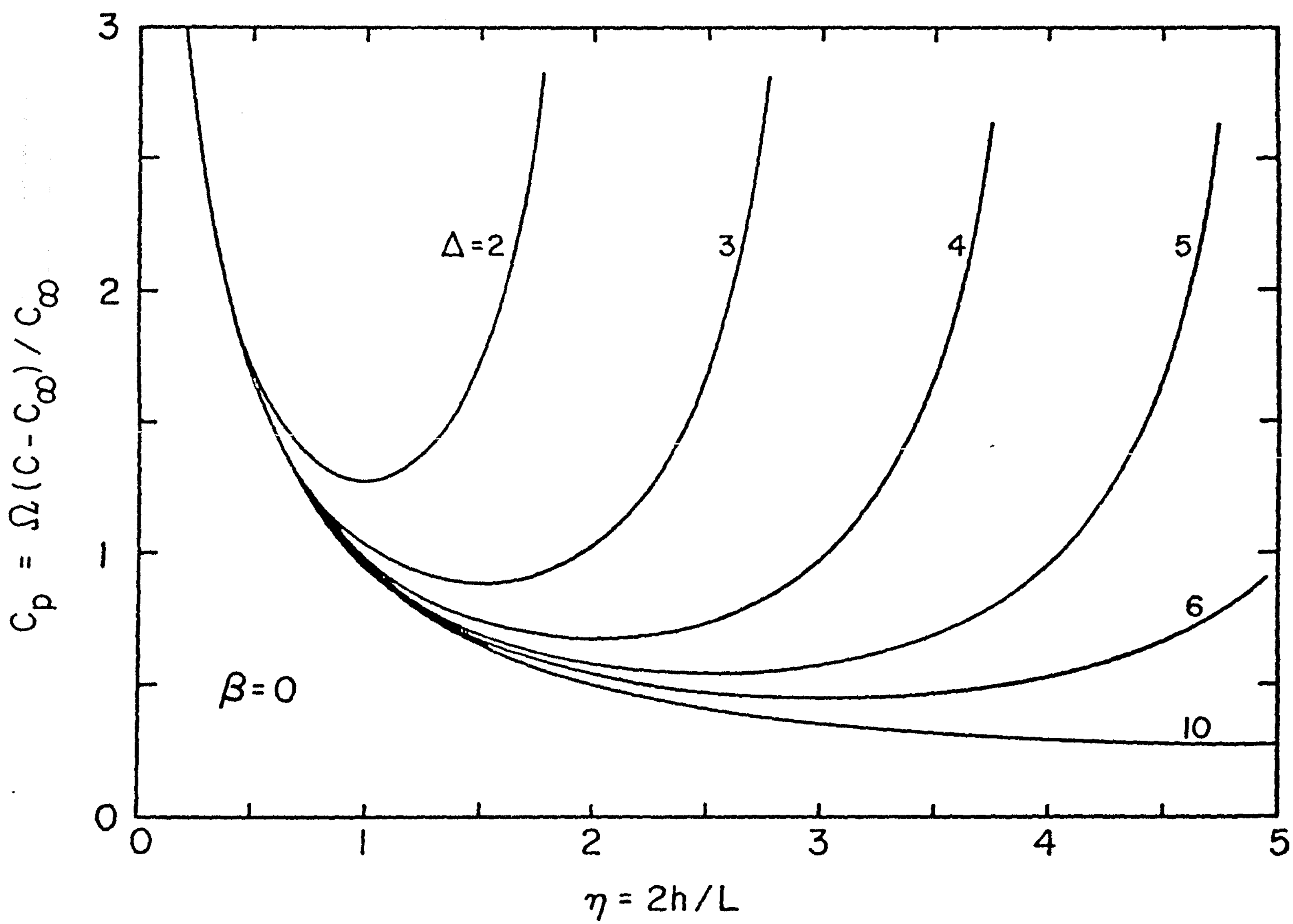

Figure 11. Variation with η of the function C_p defined by equation (13.b) for $\beta = 0$ and $\Delta \equiv 2d/L = 2,3,4,5,6,10$.

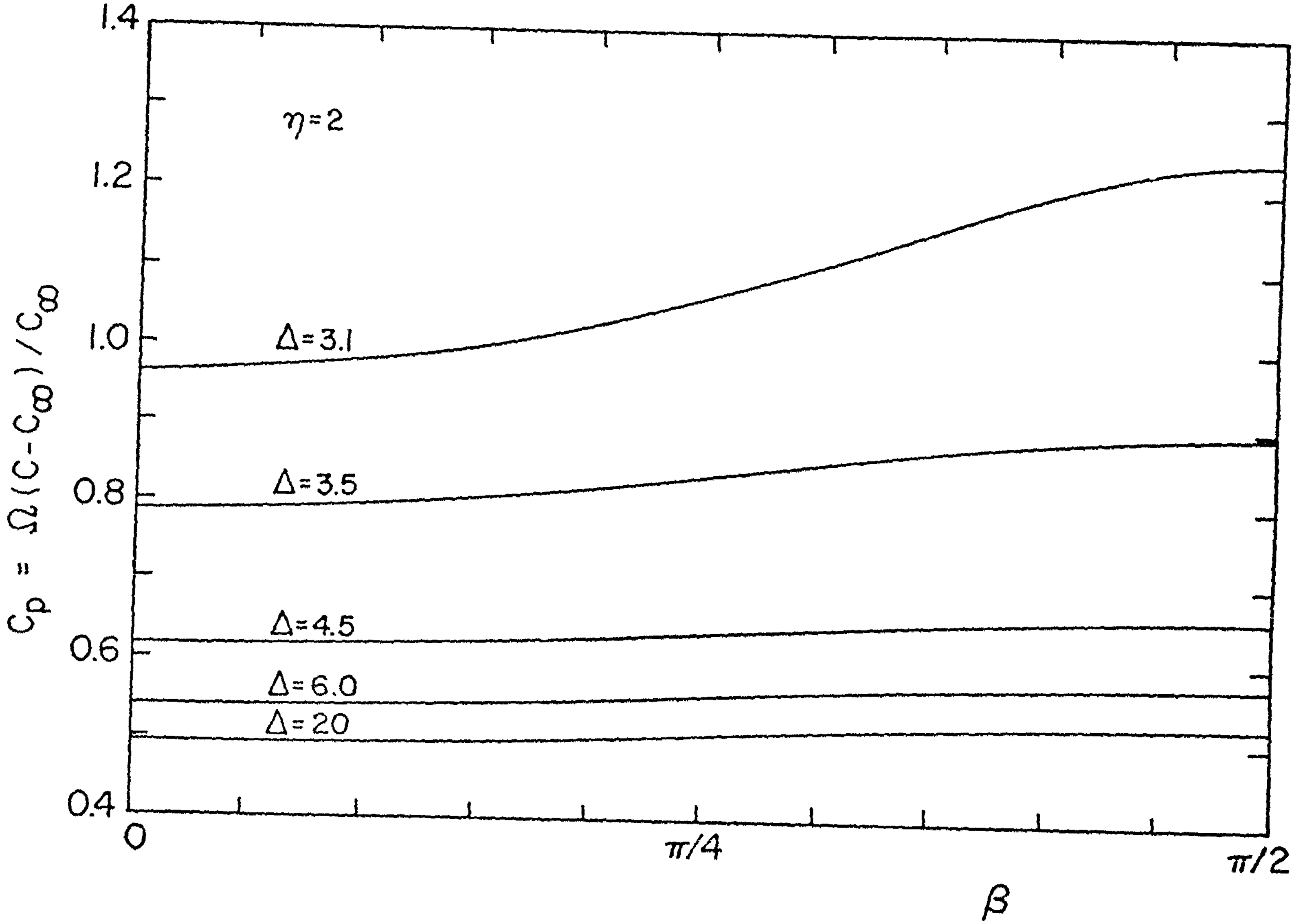

Figure 12. Variation with β of the function C_p defined by equation (13.b) for $\eta = 2h/L = 2$ and $\Delta \equiv 2d/L = 3.1, 3.5, 4.5, 6, 20$.

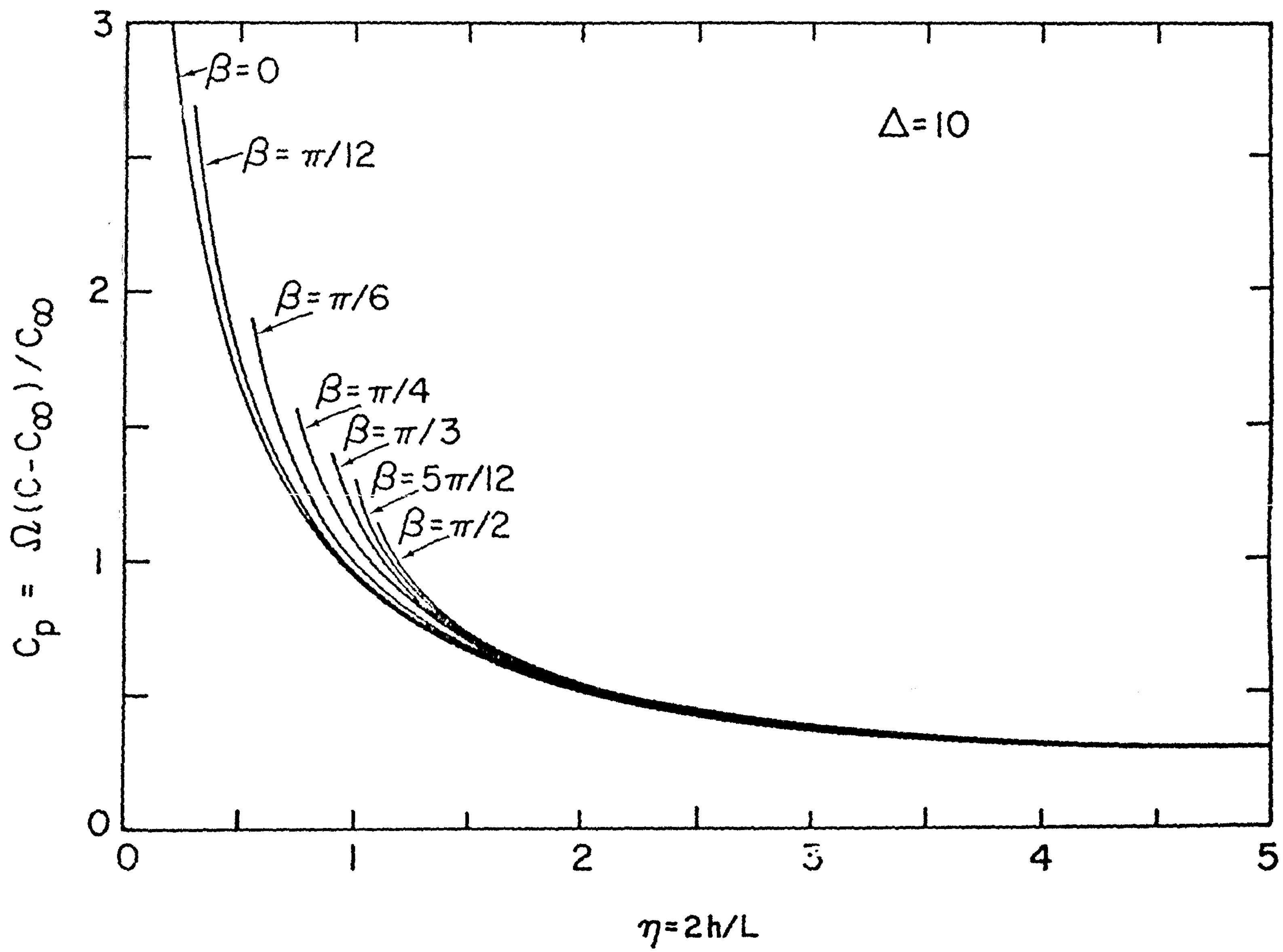

Figure 13. Variation with η of the function C_p defined by equation (13.b) for $\Delta \equiv 2d/L = 10$ and $\beta = 0, \pi/12, \pi/6, \pi/4, \pi/3, 5\pi/12, \pi/2$.

REFERENCES

[1] R.W. Latham and K.S.H. Lee, "Electromagnetic Interaction Between a Cylindrical Post and a Two-Parallel-Plate Simulator, I," EMP Sensor and Simulation Notes, Note 111, July 1970.

[2] L. Marin, "A Cylindrical Post Above a Perfectly Conducting Plate, I(Static Case)," EMP Sensor and Simulation Notes, Note 134, July 1971.

[3] F.M. Tesche, "Numerical Determination of the Step Wave Response of a Thin-Wire Scattering Element Arbitrarily Located Above a Perfectly Conducting Ground Plane," EMP Sensor and Simulation Notes, Note 141, February 1972.

[4] T.H. Shumpert, "EMP Interaction with a Thin Cylinder Above a Ground Plane Using the Singularity Expansion Method," EMP Sensor and Simulation Notes, Note 182, June 1973.

[5] L. Marin, "Natural Modes of Certain Thin-Wire Structures," EMP Interaction Notes, Note 186, August 1974.

[6] M. Abramowitz and I.N. Stegun, Editors, Handbook of Mathematical Functions, National Bureau of Standards, AMS-55, 1964.